Fig. 2. Average probability of the three ions to be measured in $|\downarrow, 3\rangle$ as a function of the offset phase ϕ_2. The fringes show a sinusoidal oscillation with period $2\pi/3$ and fringe contrast 0.84(1). deg, degrees.

During the detection period, we obtained on average 0.2 counts after preparing the state $|\uparrow, 3\rangle$ and 30 counts after preparing the state $|\downarrow, 3\rangle$. If the number of counts after a spectroscopy experiment was below 15, we assumed the outcome to be $|\uparrow, 3\rangle$; otherwise, we assumed the outcome to be $|\downarrow, 3\rangle$. The fringes resulting from averaging 1000 such experiments show a sinusoidal oscillation with period length $2\pi/3$ (Fig. 2). The fringe contrast (0.84(1)) yields a phase sensitivity that is $0.84 \times \sqrt{3} = 1.45(2)$ as high as that of a perfect Ramsey experiment with three unentangled particles. With perfect operations and readout, the method would yield a fringe contrast equal to 1 and thus reach the Heisenberg limit, giving an increase of phase sensitivity of $\sqrt{3}$ $(=\sqrt{N})$.

The gain obtained by using GHZ states can be offset by the corresponding faster decoherence if the free precession time is comparable to the dephasing time (28). However, the Ramsey time is often limited by other practical considerations, such as the desire to servo an oscillator to an atomic transition in a time that is much shorter than the decoherence time or by limitations imposed by the spectrum of the oscillator that drives the transitions (29, 30). In those cases, the entanglement provided by generalized GHZ states gives the expected gain.

We prepared a GHZ state of three atomic ions with a fidelity of 0.89(3). We used this state to demonstrate a new method for precision spectroscopy on entangled particles that can reach the Heisenberg limit and is of practical use because of its immunity to errors in final state detection. Because only collective ensemble preparation and detection pulses are used, the extension of the method to larger numbers of particles (N) is straightforward. For large values of N, the required interaction proportional to J_x^2 can be implemented with either the approach described in (10) or by further generalization of the phase gate because the operators $e^{i\chi J_x^2}$ and $e^{i\chi J_z^2}$ are equivalent up to a rotation

applied uniformly on all ions. We want the phase-space-displacement dipole forces on all ions (in the same state) to be the same, which is the case in a one-dimensional (or two-dimensional) array of trapped ions, if the forces act on a center-of-mass mode whose motion is perpendicular to the ion string (or plane) (31). The readout is robust against noise because the observable is a two-state "all-on" versus "all-off" signal. Despite experimental imperfections, our demonstration of the method on three ions shows a gain of 45% over that of a perfect Ramsey experiment with non-entangled states.

References and Notes

1. N. F. Ramsey, *Molecular Beams* (Oxford Univ. Press, London, 1956).
2. W. M. Itano et al., *Phys. Rev. A.* 47, 3554 (1993).
3. D. J. Wineland, J. J. Bollinger, W. M. Itano, D. J. Heinzen, *Phys. Rev. A.* 50, 67 (1994).
4. W. Heisenberg, *Z. Phys.* 43, 172 (1927).
5. J. J. Bollinger, W. M. Itano, D. J. Wineland, D. J. Heinzen, *Phys. Rev. A.* 54, R4649 (1996).
6. B. Yurke, S. L. McCall, J. R. Klauder, *Phys. Rev. A.* 33, 4033 (1986).
7. D. J. Wineland, J. J. Bollinger, W. M. Itano, F. L. Moore, D. J. Heinzen, *Phys. Rev. A.* 46, R6797 (1992).
8. M. Kitagawa, M. Ueda, *Phys. Rev. A.* 47, 5138 (1993).
9. A. Kuzmich, K. Mølmer, E. S. Polzik, *Phys. Rev. Lett.* 79, 4782 (1997).
10. K. Mølmer, A. Sørensen, *Phys. Rev. Lett.* 82, 1835 (1999).
11. J. Hald, J. L. Sørensen, C. Schori, E. S. Polzik, *Phys. Rev. Lett.* 83, 1319 (1999).
12. G. J. Milburn, S. Schneider, D. F. V. James, in *Scalable Quantum Computers*, S. L. Braunstein, H. K. Lo, P. Kok, Eds. (Wiley-VCH, Berlin, 2001), pp. 31–40.
13. V. Meyer et al., *Phys. Rev. Lett.* 86, 5870 (2001).
14. J. M. Geremia, J. K. Stockton, H. Mabuchi, *Science* 304, 270 (2004).
15. X. Wang, A. Sørensen, K. Mølmer, *Phys. Rev. Lett.* 86, 3907 (2001).
16. D. Leibfried et al., *Nature* 422, 412 (2003).
17. M. J. Holland, K. Burnett, *Phys. Rev. Lett.* 71, 1355 (1993).
18. P. Bouyer, M. A. Kasevich, *Phys. Rev. A.* 56, R1083 (1997).
19. D. M. Greenberger, M. A. Horne, A. Shimony, A. Zeilinger, *Am. J. Phys.* 58, 1131 (1990).
20. C. A. Sackett et al., *Nature* 404, 256 (2000).
21. A. Steane, *Proc. R. Soc. Lond. Ser. A* 452, 2551 (1996).
22. H. G. Dehmelt, *IEEE Trans. Inst. Meas.* 31, 83 (1982).
23. M. A. Rowe et al., *Quantum Inf. Comput.* 2, 257 (2002).
24. B. E. King et al., *Phys. Rev. Lett.* 81, 1525 (1998).
25. The rotations could also be induced directly with radiation at ω_0. This can be an advantage because of the technical difficulty of maintaining a precise frequency difference between Raman beams for large ω_0.
26. D. J. Wineland et al., *Philos. Trans. R. Soc. Lond. Ser. A* 361, 1349 (2003).
27. In general we can write $G = \exp[i\xi(J_z^2 + NJ_z(F_\uparrow + F_\downarrow)/(F_\uparrow - F_\downarrow))]$ where ξ is a phase factor and F_i is the optical dipole force on state $|i\rangle$. For the experiments here, $F_\downarrow = -2F_\uparrow$.
28. S. F. Huelga et al., *Phys. Rev. Lett.* 79, 3865 (1997).
29. D. J. Wineland et al., *J. Res. Natl. Inst. Stand. Technol.* 103, 259 (1998).
30. A. Andre, A. S. Sørensen, M. D. Lukin, preprint available at http://arxiv.org/abs/quant-ph/0401130.
31. Dipole-force phase gates have the disadvantage that they can be ineffective when, for example, implemented on magnetic field–insensitive hyperfine transitions.
32. Supported by the U.S. National Security Agency (NSA) and Advanced Research and Development Activity (ARDA) and by NIST. We thank J. Bollinger and E. Knill for comments on the manuscript. This paper is a contribution by the National Institute of Standards and Technology and not subject to U.S. copyright.

Control and Measurement of Three-Qubit Entangled States

Christian F. Roos,[1] **Mark Riebe,**[1] **Hartmut Häffner,**[1]
Wolfgang Hänsel,[1] **Jan Benhelm,**[1] **Gavin P. T. Lancaster,**[1]
Christoph Becher,[1] **Ferdinand Schmidt-Kaler,**[1*] **Rainer Blatt**[1,2]

We report the deterministic creation of maximally entangled three-qubit states—specifically the Greenberger-Horne-Zeilinger (GHZ) state and the W state—with a trapped-ion quantum computer. We read out one of the qubits selectively and show how GHZ and W states are affected by this local measurement. Additionally, we demonstrate conditional operations controlled by the results from reading out one qubit. Tripartite entanglement is deterministically transformed into bipartite entanglement by local operations only. These operations are the measurement of one qubit of a GHZ state in a rotated basis and, conditioned on this measurement result, the application of single-qubit rotations.

Quantum information processing rests on the ability to deliberately initialize, control, and manipulate a set of quantum bits (qubits) forming a quantum register (1). Carrying out an algorithm then consists of sequences of quantum gate operations that generate multipartite entangled states of this quantum register. Eventually, the outcome of the computation is obtained by measuring the state of the individual qubits. For the realization of some important algorithms such as quantum error correction (1–5) and teleportation (6), a subset of the quantum register must be read out selectively, and subsequent operations on other qubits must be conditioned on the measurement result. The capability of entangling a scalable quantum register is the key ingredient for quantum information processing as well as for many-party quantum communication. Whereas entanglement with two or more

qubits has been demonstrated (7–13), our experiment allows the deterministic generation of three-qubit entangled states and the selective readout of an individual qubit followed by local quantum operations conditioned on the readout.

The experiments are performed in an elementary ion-trap quantum processor (14, 15). For the investigation of tripartite entanglement (16–18), we trap three $^{40}Ca^+$ ions in a linear Paul trap. Qubits are encoded in a superposition of the $S_{1/2}$ ground state and the metastable $D_{5/2}$ state (lifetime $\tau \approx 1.16$ s). Each ion-qubit is individually manipulated by a series of laser pulses on the $S \equiv S_{1/2}$ ($m_j = -1/2$) to $D \equiv D_{5/2}$ ($m_j = -1/2$) quadrupole transition near 729 nm, with the use of narrow-band laser radiation tightly focused onto individual ions in the string. The entire quantum register is prepared by Doppler cooling, followed by sideband ground-state cooling of the center-of-mass vibrational mode ($\omega = 2\pi \times 1.2$ MHz). The ions' electronic qubit states are initialized in the S state by optical pumping.

Three qubits can be entangled in only two inequivalent ways, represented by the Greenberger-Horne-Zeilinger (GHZ) state, $|GHZ\rangle = (|SSS\rangle + |DDD\rangle)/\sqrt{2}$, and the W state, $|W\rangle = (|DDS\rangle + |DSD\rangle + |SDD\rangle)/\sqrt{3}$ (17). The W state can retain bipartite entanglement when any one of the three qubits is measured in the $\{|S\rangle, |D\rangle\}$ basis, whereas for the maximally entangled GHZ state a measurement of any one qubit destroys the entanglement. We synthesize the GHZ state with a sequence of 10 laser pulses and the W state with a sequence of five laser pulses (19).

Full information on the three-ion entangled states is obtained by state tomography (20, 21) using a charge-coupled device camera for the individual detection of ions. The pulse sequences generate three-ion entangled states within less than 1 ms. Determining all 64 entries of the density matrix with an uncertainty of less than 2% requires about 5000 experiments, corresponding to 200 s of measurement time.

In the experimental results for the absolute values of the density matrix elements of GHZ and W states, $\rho_{|GHZ\rangle}$ and $\rho_{|W\rangle}$ (Fig. 1, A and B), the off-diagonal elements are observed with heights nearly equal to those of the corresponding diagonal elements and with the correct phases (19). Fidelities of 72% for $\rho_{|GHZ\rangle}$ and 83% for $\rho_{|W\rangle}$ are ob-

tained. The fidelity is defined as $|\langle\Psi_{ideal}|\rho_{exp}|\Psi_{ideal}\rangle|^2$, where Ψ_{ideal} denotes the ideal quantum state and ρ_{exp} is the experimentally determined density matrix. All sources of imperfection have been investigated independently (14) and the measured fidelities are consistent with the known error budget. Note that for the W state, coherence times greater than 200 ms were measured (exceeding the synthesis time by almost three orders of magnitude), whereas for the GHZ state only times of ~1 ms were found. This is because the W states are a superposition of three states with the same energy. Thus, the dephasing due to magnetic field fluctuations is much reduced in contrast to a GHZ state that is maximally sensitive to such perturbations. Similar behavior has been observed with Bell states (21, 22).

Having tripartite entangled states available as a resource, we make use of individual ion addressing to read out only one of the three ions' quantum state while preserving the coherence of the other two. Qubits are protected from being measured by transferring their quantum information into superpositions of levels that are not affected by the detection—that is, by a light-scattering pro-

cess. In Ca^+, an additional Zeeman level D' $\equiv D_{5/2}$ ($m = -5/2$) can be used for this purpose. Thus, after the state synthesis, we apply two π pulses on the S-D' transition of ions 2 and 3, moving any S population of these ions into their respective D' level. The D and D' levels do not couple to the detection light at 397 nm (Fig. 2). Therefore, ion 1 can be read out by the electron shelving method as usual (15). After the selective readout, a second set of π-pulses on the D'-S transition transfers the quantum information back into the original computational subspace {S, D}.

For a demonstration of this method, GHZ and W states are generated and qubits 2 and 3 are mapped onto the {D, D'} subspace. Then, the state of ion 1 is projected onto S or D by scattering photons for a few microseconds on the S-P transition. In a first series of experiments, we did not distinguish whether ion 1 was projected into S or D. After remapping qubits 2 and 3 to the original subspace {S, D}, the tomography procedure is applied to obtain the full density matrix of the resulting three-ion state. As shown in Fig. 1C, the GHZ state is completely destroyed; that is, it is projected into a mixture of $|SSS\rangle$ and $|DDD\rangle$. In
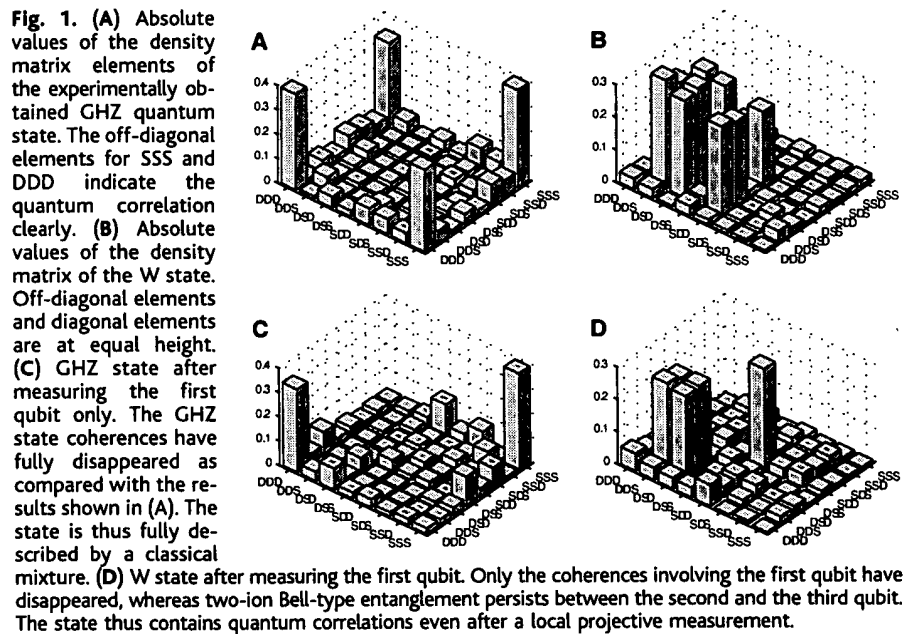
Fig. 1. (A) Absolute values of the density matrix elements of the experimentally obtained GHZ quantum state. The off-diagonal elements for SSS and DDD indicate the quantum correlation clearly. (B) Absolute values of the density matrix of the W state. Off-diagonal elements and diagonal elements are at equal height. (C) GHZ state after measuring the first qubit only. The GHZ state coherences have fully disappeared as compared with the results shown in (A). The state is thus fully described by a classical

mixture. (D) W state after measuring the first qubit. Only the coherences involving the first qubit have disappeared, whereas two-ion Bell-type entanglement persists between the second and the third qubit. The state thus contains quantum correlations even after a local projective measurement.
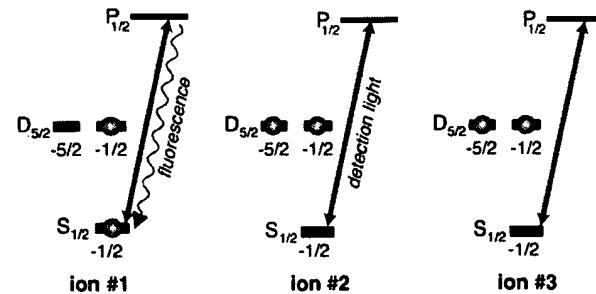

Fig. 2. Selective readout of ion 1: Ions 2 and 3 are protected from measurement by transfer into dark states. Only the relevant levels of the three Ca^+ ions are shown.

[1]Institut für Experimentalphysik, Universität Innsbruck, Technikerstraße 25, A-6020 Innsbruck, Austria. [2]Institut für Quantenoptik und Quanteninformation, Österreichische Akademie der Wissenschaften, Technikerstraße 25, A-6020 Innsbruck, Austria.

*To whom correspondence should be addressed. E-mail: ferdinand.schmidt-kaler@uibk.ac.at

contrast, for the W state, the quantum register remains partially entangled as coherences between ions 2 and 3 persist (Fig. 1D). Related experiments have been carried out with mixed states in nuclear magnetic resonance (13) and with photons (11).

In a second series of experiments with the W state, we deliberately determined the first ion's quantum state before tomography: The ion string is now illuminated for 500 μs with light at 397 nm, and its fluorescence is collected with a photomultiplier tube (Fig. 3A). Then the state of ion 1 is known, and we subsequently apply the tomographic procedure to ions 2 and 3 after remapping them to their {S, D} subspace. Depending on the state of ion 1, we observe the two density matrices presented in Fig. 3, B and C (19). Whenever ion 1 was measured in D, ions 2 and 3 were found in a Bell state $[(|SD\rangle + |DS\rangle)/\sqrt{2}]$, with a fidelity of 82%. If the first qubit was observed in S, the resulting state is $|DD\rangle$ with fidelity of 90%. This is a characteristic signature of $W = (|DDS\rangle + |DSD\rangle + |SDD\rangle)/\sqrt{3}$: In one-third of the cases, the measurement projects qubit 1 into the S state, and consequently the other two qubits are projected into D. With a probability of 2/3, however, the measurement shows qubit 1 in D, and the remaining quantum register is found in a Bell state (17). Experimentally, we observe the first ion in D in 65 ± 2% of the cases.

The GHZ state can be used to deterministically transform tripartite entanglement into bipartite entanglement by means of only local measurements and one-qubit operations. For this, we first generate the GHZ state $(|DSD\rangle + |SDS\rangle)/\sqrt{2}$. In a second step, we apply a π/2 pulse to ion 1, with phase 3π/2, rotating a state $|S\rangle$ to $(|S\rangle - |D\rangle)/\sqrt{2}$ and $|D\rangle$ to $(|S\rangle + |D\rangle)/\sqrt{2}$, respectively. The resulting state of the three ions is $\{|D\rangle(|SD\rangle - |DS\rangle) + |S\rangle(|SD\rangle + |DS\rangle)\}/\sqrt{2}$. A measurement of the first ion, resulting in $|D\rangle$ or $|S\rangle$, projects qubits 2 and 3 onto the state $(|SD\rangle - |DS\rangle)/\sqrt{2}$ or the state $(|SD\rangle + |DS\rangle)/\sqrt{2}$, respectively. The corresponding density matrix is plotted in Fig. 4A. With the information on the state of ion 1 available, we can now transform this mixed state into the pure state $|S\rangle(|SD\rangle + |DS\rangle)/\sqrt{2}$ by only local operations. Provided that ion 1 is found in $|D\rangle$, we perform an appropriate rotation (19) on ion 2 to obtain $|D\rangle(|SD\rangle + |DS\rangle)/\sqrt{2}$. In addition, we flip the state of ion 1 to reset it to $|S\rangle$. Figure 4B shows that the bipartite entangled state $|S\rangle(|SD\rangle + |DS\rangle)/\sqrt{2}$ is produced with fidelity of 75% (19). This procedure can also be regarded as an implementation of a three-spin quantum eraser, as proposed in (23).

Our results show that selectively reading out a qubit of the quantum register indeed leaves the entanglement of all other qubits in the register untouched. Even after such a measurement has taken place, single-qubit rotations can be performed with high fidelity. Such techniques represent a step toward the one-way quantum computer (24). The implementation of unitary transformations conditioned on measurement results allows for the realization of deterministic quantum teleportation and of active quantum error correction algorithms. With further improvements of the gate fidelity, it will be possible to realize two different protocols for quantum error correction— either to perform a strong measurement on the ancilla qubit and to rotate the target qubit correspondingly or, alternatively, to rotate the target qubit conditional upon the still-unknown ancilla quantum state by conditional gate operations and to reset the ancilla afterward. It remains to be determined which of the two methods is favorable for our setup.

References and Notes

1. M. Nielsen, I. Chuang, Quantum Computation and Quantum Information (Cambridge Univ. Press, New York, 2000).
2. P. W. Shor, Phys. Rev. A 52, R2493 (1995).
3. A. M. Steane, Phys. Rev. Lett. 77, 793 (1996).
4. C. H. Bennett, D. P. DiVincenzo, J. A. Smolin, W. K. Wootters, Phys. Rev. A 54, 3824 (1996).
5. A. M. Steane, Nature 399, 124 (1999).
6. C. H. Bennet, Phys. Rev. Lett. 70, 1895 (1993).
7. A. Rauschenbeutel et al., Science 288, 2024 (2000).
8. C. A. Sackett et al., Nature 404, 256 (2000).
9. J. W. Pan, D. Bouwmeester, M. Daniell, H. Weinfurter, A. Zeilinger, Nature 403, 515 (2000).
10. J. W. Pan, M. Daniell, S. Gasparoni, G. Weihs, A. Zeilinger, Phys. Rev. Lett. 86, 4435 (2001).
11. M. Eibl, N. Kiesel, M. Bourennane, C. Kurtsiefer, H. Weinfurter, Phys. Rev. Lett. 92, 077901 (2004).
12. Z. Zhao et al., http://arXiv.org/abs/quant-ph/0402096 (2004).
13. G. Teklemariam et al., Phys. Rev. A 66, 012309 (2002).
14. F. Schmidt-Kaler et al., Nature 422, 408 (2003).
15. F. Schmidt-Kaler et al., Appl. Phys. B 77, 789 (2003).
16. D. M. Greenberger, M. Horne, A. Zeilinger, in Bell's Theorem, Quantum Theory, and Conceptions of the Universe, M. Kafatos, Ed. (Kluwer Academic, Dordrecht, Netherlands, 1989), pp. 73–76.
17. W. Dür, G. Vidal, J. I. Cirac, Phys. Rev. A 62, 062314 (2000).
18. A. Zeilinger, M. A. Horne, D. M. Greenberger, NASA Conf. Publ. 3135 (NASA, Washington, DC, 1997).
19. See supporting data on Science Online.
20. D. F. V. James, P. G. Kwiat, W. J. Munro, A. G. White, Phys. Rev. A 64, 052312 (2001).
21. C. F. Roos et al., Phys. Rev. Lett., in press; available at http://arXiv.org/abs/quant-ph/0307210 (2003).
22. D. Kielpinski et al., Science 291, 1013 (2001).
23. R. Garisto, L. Hardy, Phys. Rev. A 60, 827 (1999).
24. R. Raussendorf, H. J. Briegel, Phys. Rev. Lett. 86, 5188 (2001).
25. Supported by the European Commission (QUEST and QGATES networks), the Army Research Office, the Austrian Science Fund (FWF), and the Institut für Quanteninformation GmbH. H.H. was supported by the Marie Curie program of the European Union. We thank A. Steinberg, D. F. V. James, and H. Briegel for discussions.

Fig. 3. (A) Histogram of photon counts within 500 μs for ion 1 and threshold setting. (B and C) Density matrix of ions 2 and 3 conditioned on the previously determined quantum state of ion 1. The absolute values of the reduced density matrix are plotted for ion 1 measured in the S state (B) and ion 1 measured in the D state (C). Off-diagonal elements in (B) show the remaining coherences.
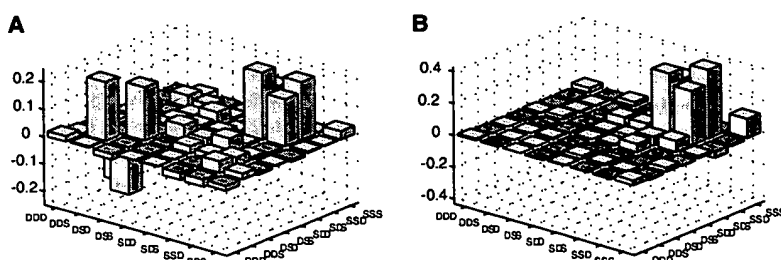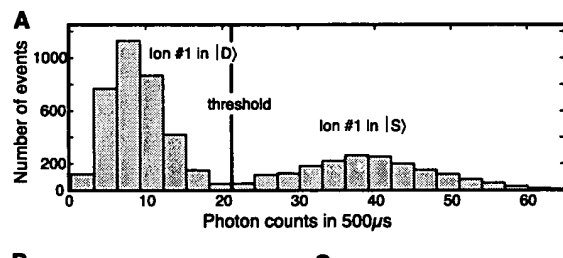

Fig. 4. (A) Real part of the density matrix elements of the system after ion 1 of the GHZ state $(|DSD\rangle + |SDS\rangle)/\sqrt{2}$ has been measured in a rotated basis. (B) Transformation of the GHZ state $(|DSD\rangle + |SDS\rangle)/\sqrt{2}$ into the bipartite entangled state $|S\rangle(|DS\rangle + |SD\rangle)/\sqrt{2}$ by conditional local operations. Note the different vertical scaling of (A) and (B).